Heterogeneous & Homogeneous & Bio- & Nano-
CHEMCATCHEM
CATALYSIS

Accepted Article

Title: A Serendipitous Observation of Liquid Phase Size Selectivity inside Mesoporous Silica Nanoreactor in the Reaction of Chromene with Formic Acid

Authors: Paramita Das, Suman Ray, Piyali Bhanja, Asim Bhaumik, and Chhanda Mukhopadhyay

To be cited as: *ChemCatChem* 10.1002/cctc.201701975

Link to VoR: http://dx.doi.org/10.1002/cctc.201701975

A Journal of
ChemPubSoc Europe

WILEY-VCH

www.chemcatchem.org

A Serendipitous Observation of Liquid Phase Size Selectivity inside Mesoporous Silica Nanoreactor in the Reaction of Chromene with Formic Acid

Paramita Das,[a] [b] Suman Ray,[a] Piyali Bhanja,[c] Asim Bhaumik,[c] and Chhanda Mukhopadhyay*[a]

Abstract: Unprecedented sharp product shape/size selectivity in the hydrolysis/decarboxylation reaction sequences of chromene with formic acid within MCM-41 as nanoreactor in liquid phase is observed. Chromeneis expected to form pyrimidine in the reaction with HCOOH. However, here, serendipitously the product switches from pyrimidine to enol lactones and δ-keto acids inside nanoreactor. The shape/size selectivity in liquid medium is a highly desired phenomenon in organic synthesis. We have prepared four different varieties of porous silica materials to fetch this product selectivity. Very high yields of these biologically relevant compound surpass the existing methodologies. Again, though there are few reports of coumarin-fused enol lactone, this approach enables the easy synthesis of naphthalene-fused enol lactones which is rarely reported. Moreover, this is the first generalized synthesis of δ-keto acids following a number of hydrolysis/decarboxylation/ring opening/tautomerization/decarboxylation steps.

Introduction

Selectivity in organic synthesis continues to be one of the key concerns of the synthetic chemists. Of the various strategies employed, the use of nanoreactors to control the product selectivity has shown significant prospects.[1] Two main types of selectivities are frequently practiced in the design of nanoreactors, either the preferential formation of a particular molecule among two or more possible products or the preference for one of the stereoisomers.[2] The term nanoreactor indicates a constrained and organized space where the chemical reactions occur. It is previously demonstrated that organic photochemical reactions inside nanoreactors show deviance in product distribution and follow reaction pathways that are not otherwise seen.[1] Selectivities in organic synthesis has been achieved inside nanoreactors in different organic transformations including but not limited to chemoselective oxidations and reductions, hydrogenations and C-C bond-formation reactions etc.[2] This effect stems from (i) selective ingress of guest molecules inside nanoreactor according to size/shape of the molecules, (ii) diffusion barrier caused by the nanoreactor, and (iii) restriction imposed by the nanoreactor on rotational and translational motions of the included guest molecules and intermediates or products.[3] Both the effects depend on size and shape of the molecules accommodated inside nanoreactor. Owing to the impact of nanoreactor on product selectivities, the efficacious design of nanoreactors may provide efficient tools for performing organic reactions in a selective and very competent way. Again, the mesoporous materials provide a size/shape and functional group selective microenvironment that allows encapsulation of guest molecules for confined synthesis and catalysis.[4] In this context, ordered mesoporous silicas[5-10] having highly ordered pore structures, high specific surface area, tunable morphology, and high thermal stability have enthused significant research efforts in shape-selective heterogeneous catalysis.[11] The pores that control the transport pathways act as a diffusion barrier to reactants and products and consequently impact on the product selectivity. The morphological features of silica have been known to influence the hydrocarbon selectivity in Fischer-Tropsch synthesis.[12] For example, SBA-15 with large pore diameter (6-10 nm) was reported to have heavy hydrocarbon selectivity whereas short-pore SBA-15 has C5+ selectivity.[12,13] Chen et al. have recently reported the shape selectivity of a Suzuki cross-coupling reaction using mesopores Pd on mesoporous silica as nanoreactors in liquid medium.[3] Furthermore, in heterogeneous asymmetric catalysis, the effect of pore confinement on improving enantoselectivity has been studied.[14] Despite this breakthrough, achieving size/shape selectivity in liquid phase in organic synthesis using nanoreactor is an appealing approach and a fascinating theme. In this study, we observed unprecedented sharp product shape/size selectivity in the reaction of chromene with formic acid within the mesoporous pores of MCM-41 nanoreactor and it occurred in liquid phase.

"The design of chemical products and processes that reduce or eliminate the use or generation of hazardous substances" fosters the principle and practice of sustainable chemistry, as defined by U.S. Environmental Protection Agency (EPA).[15,16] The most pivotal area of chemistry dealing with the development of medicinally and pharmaceutically relevant molecules, with their traditionally large volume of waste/product ratio, is perhaps most ripe for sustainability.[17] In addition, it is possible to apply the tenets of sustainability to the generation of biologically interesting products using aqueous medium approaches. Therefore, development of synthetically useful, elegant and convergent reactions in water is appealing to an environmentally cognizant society. Again "Organocatalysis" has

[a] P.Das, S. Ray, C.Mukhopadhyay
Department of Chemistry, University of Calcutta,
92, APC Road, Kolkata-700009, India.
*Tel: +91-9433019610; *Email: cmukhop@yahoo.co.in
[b] P. Das
Asutosh College
Department of Chemistry
92, S. P. Mukherjee Road, Kolkata-700026, India
[c] A. Bhaumik, P.Bhanja
Department of Materials Science,
Indian Association for the Cultivation of Science, Jadavpur,
Kolkata-700032, India

Supporting information for this article is given via a link at the end of the document (CCDC: 1408025, 1408026, 1407896, 1407897,1407898, and 1408296).

emerged during the last decade as one of the major issues in the development of catalytic chemical technology because of its suntainibility perspectives and analogy to eon-perfected enzyme catalysis.[18] Organocatalytic methods are especially attractive for the preparation of compounds that must not tolerate metal contamination, such as pharmaceutically relevant molecules.[19] Thus, the challenge of developing efficient aqueous-phase organocatalytic processes has been posed.[20]

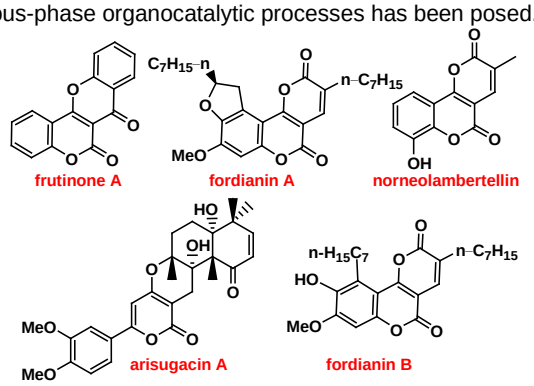

Figure 1. Significant examples of biologically active enol lactones.

Naturally occurring biologically active molecules are outstanding source of lead compounds in drug disocovery.[21] Enol lactones, such as the derivatives of coumarin,[22] flavonoids,[23] and neoflavonoids,[24] comprise ubiquitous structural motifs in a number of biologically active natural products.[25] In particular, annulated enol lactones exhibit outstanding natural and biological activities. For instance, frutinone A has antibacterial and antioxidant activity,[26] fordianin A and fordianin B have cytotoxicity against A549 (human lung cancer) and human cervical carcinoma,[27] norneolambertellin functions as an antifungal,[28] coumestrol acts as an anti-breast cancer[27,29] and Arisugacin A possesses significance in the treatment of Alzheimer's disease[30] (Figure 1).

However, despite the importance of these compounds in the field of medicine, unexpectedly, there are only few novel reports available in the literature documenting the synthesis of enol lactones.[31] Moreover, some of the experimental conditions have not been optimized on the sustainability point of views. The most effective access to these class of compounds, so far reported, is the condensation reactions of isopropylidene malonate with aromatic aldehydes followed by the Michael addition of dimedone and/or 4-hydroxycoumarin.[32] Moreover, they suffer from the use of a limited number of C-H-activated acids, mainly, activated 1,3-diketo systems. Reports with unactivated *α*- and *β*-naphthol to produce naphthalene-fused enol lactones are even rarer,[33] which is far from the demand of diversity-oriented target synthesis. This may be due to the absence of a convenient protocol for preparing naphthalene-fused enol lactones. Kanemasa[34] and Biju[35] independently reported convenient and elegant approach towards enol lactones. Despite this advance, metal-free reaction in environmentally benign solvent using simplest catalyst and starting material is an attractive approach.

Results and Discussion

Characterization of Silica

We have prepared four different varieties of porous silica materials namely large pore MCM-41 (**LP-MCM-41**), microporous silica nano particle (**Micro-SNP**), small pore MCM-41 (**SP-MCM-41**) and mesoporous silica nano particle (**Meso-SNP**). Among them small pore MCM-41 (**SP-MCM-41**) andmesoporous silica nano particle (**Meso-SNP**) worked efficiently as a size selective reaction vessel for preferential formation of enol lactones instead of pyrimidine in the reaction of chromene with HCOOH. The characterizations of these two materials are given below. Characterizations of the other two materials are presented in Supporting Information I.

Nitrogen adsorption analysis.

Nitrogen adsorption analysis has been carried out using a Quantachrome Autosorb 1-C surface area analyzer at 77 K after outgassing the samples at 130 °C under high vacuum. Figure 2a represents the N_2 adsorption-desorption isotherm of **SP-MCM-41** which is classified as typical type IV isotherm with H4 hysteresis loop according to IUPAC nomenclature. In Figure 2a, the capillary condensation at a relatively low partial pressure (P/P_0) region of 0.05 to 0.23 of nitrogen, indicates the presence of small mesopores.[36] The material exhibits H4 hysteresis loop at high pressure region 0.46-0.98 bar, suggesting the existence of uniform large pore size throughout the whole material. The BET (Brunauer-Emmett-Teller) surface area of **SP-MCM-41** was found to be 833 m^2g^{-1}. For **Meso-SNP** irreversible type IV adsorption isotherm with H1 hysteresis loop are observed, that is a typical characteristic of mesoporous materials (Figure 2c). BET Surface area was calculated to be 556 m^2g^{-1}. This is a reasonably high value and also a characteristic feature of **MCM-41** type silica materials. The pore volume of **SP-MCM-41** and **Meso-SNP** were 0.386 ccg^{-1} and 0.52 ccg^{-1} respectively.

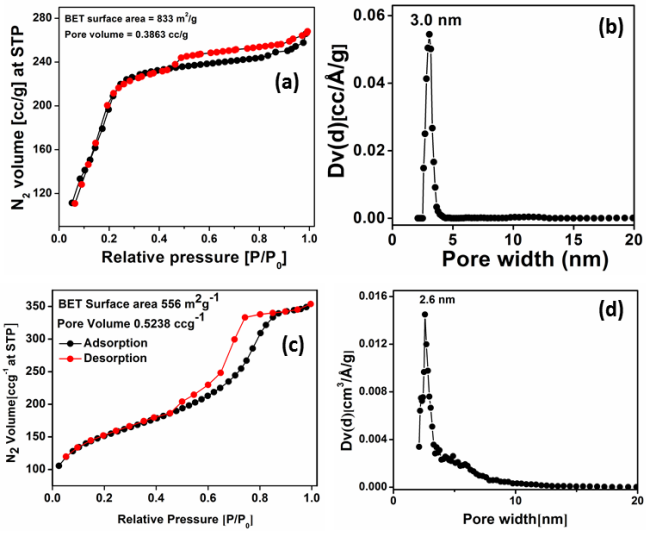

Figure 2. (a) N_2 adsorption isotherm and (b) pore size distribution of **SP-MCM-41**; (c) N_2 adsorption isotherm and (d) pore size distribution of **Meso-SNP**.

Non-Local Density Functional Theory (NLDFT) method was used to estimate the pore size distribution plots of **SP-MCM-41** and **Meso-SNP**, shown in Figure 2b and 2d respectively. A sharp peak is observed in the PSD of **SP-MCM-41** indicating uniform mesopores having dimension of 3.0 nm. This data matches well with the value obtained from UHR TEM analysis of the sample. Whereas for **Meso-SNP**, the pore size distribution is little broad with peak pore diameter of 2.6 nm.

UHR-TEM analysis

Representative UHR-TEM images of **SP-MCM-41** are shown in Figure 3a-b. In Figure 3b, regularly arranged ordered hexagonal pores which are perpendicular to the pore axis with a dimension of ~2.8 nm are clearly observed. This indicates the existence of mesoporosity in the **SP-MCM-41** material. The FFT (Fast Fourier Transform pattern) given in the inset of Figure 3b, represents the highly ordered hexagonal array of the material.

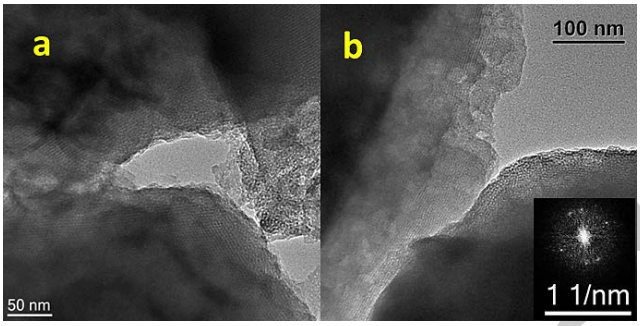

Figure 3. UHR-TEM images of **SP-MCM-41** (a, b).

Again, the UHR-TEM image analysis of **Meso-SNP** reveals that this mesoporous silica material is composed of uniform spheres having dimension of around 800 nm (Figure 4a-b). In these figures low electron density spots (pores) are seen throughout the specimen, and pores of dimensions *ca.* 2.6 nm are observed.

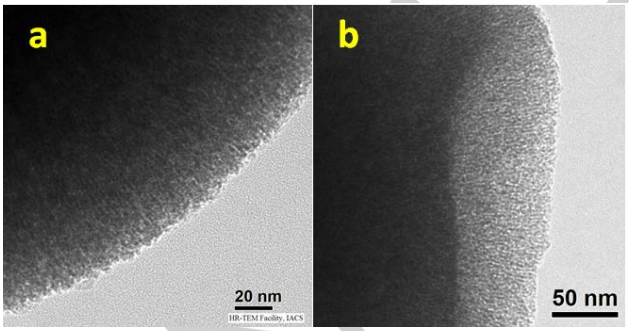

Figure 4. UHR-TEM images of **Meso-SNP** (a, b).

X-ray diffraction analysis

The small angle powder X-ray diffraction pattern of **SP-MCM-41** is shown in Figure 5a. As seen from the figure, **SP-MCM-41** material displays three characteristic diffraction peaks centered at 2θ values of 2.4, 4.2 and 4.8° which can be attributed for the distinct planes i.e.,100 (strong), 110 (weak), and 200 (weak) reflections. This implies the presence of two dimensional hexagonal mesopores.[37] However, in the small angle powder XRD pattern of **Meso-SNP** only a single peak is observed (Figure 5b). The d spacing calculated using Bragg's equation depicts the value as 3.08 nm which is in close agreement with the individual UHR-TEM analysis.

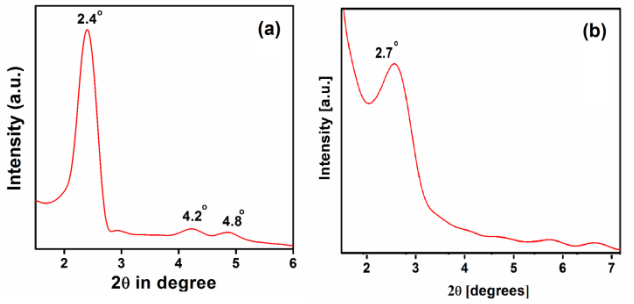

Figure 5. Small angle XRD pattern of **SP-MCM-41** (a); and **Meso-SNP** (b).

Synthetic application of nanoreactor

In our recent paper we have reported experimentally and environmentally convenient approach towards the library synthesis of 88 different chromene compounds using heterogeneous $ZnFe_2O_4$ nano-powder in water.[38] Consequently, our long-term quest was directed at exploring further application of the pyrano-chromene and benzo-chromene systems. Since the pyrimidine ring is an integral part of various natural products of therapeutic importance,[39] we therefore, first refluxed the chromenes with excess HCOOH to afford pyrimidine as stated in literature.[39a,b] But to our surprise, along with the expected pyrimidine, a trace amount of an unanticipated product was also formed (Scheme 1). Albeit, the ^{1}H NMR spectrum of the unexpected molecule was very simple, we could not unambiguously determine the structure only from NMR spectroscopy. Finally, the formation of the unanticipated enol-lactones through an unexpected triple hydrolysis/decarboxylation cascades were confirmed from X-ray single crystal analyses. Hence, we comprehended that this would be a new chemistry, and if the reaction conditions could be optimized, a novel strategy for the synthesis of enol lactones would be established.

Optimization of Reaction Conditions

Since our group is actively working for long on silica based heterogeneous catalyst[40] for greener reaction protocols and stimulated by our previous experience regarding switchable shift in product selectivity inside the silica meso/nano pores while using the same precursor, we decided to use the porous silica as a size selective nanoreactor.[40a] We anticipated that if the

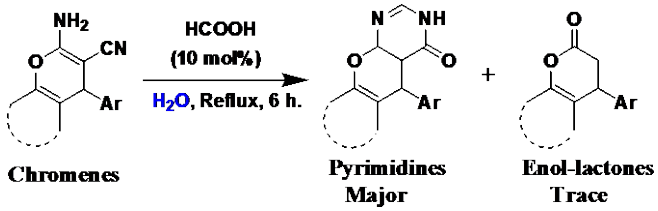

Scheme 1. The possible products formed in the reaction between chromenes and HCOOH.

reaction is performed in water, the hydrophobic organic chromene compounds will preferably enter the channels of silica since the environment inside the pores are little less hydrophilic than the sea of water outside the pores and the reaction will ensue inside the pores. Accordingly, depending on the size of pores one particular transition state or product will be favored because of the constraint imposed by the silica wall. To authenticate this proposition, a series of experiments were conducted with a representative reaction of 2-amino-4-(4-nitrophenyl)-5-oxo-4*H*,5*H*-pyrano[3,2-*c*]chromene-3-carbonitrile (**1f**) in presence of four different porous silica materials with varied pore diameter, pore volume and surface area (Table 1). The chromene derivative (**1f**) was first refluxed with excess of HCOOH in water at 100 °C in presence of large pore MCM-41 (**LP-MCM-41**) with pore diameter 3.56 nm and pore volume 1.79 ccg^{-1}. Disappointingly, we isolated the pyrimidine compound (**P**) as the exclusive product (Table 1, entry 2). Therefore, we assumed that large pore silica as reaction vessel could not impose any product selectivity by preferentially stabilizing one particular transient state or product. Keeping this in mind we next prepared microporous silica (**Micro-SNP**) with pore diameter 1.0-1.2 nm and pore volume 0.65 ccg^{-1} instead of mesoporous silica with large pore diameter. Yet again we isolated only the pyrimidine compound (Table 1, entry 3). We understood that in this instance, the reaction might have taken place at the external surface of the particles, since ingress of starting materials was not possible through these small pores thereby, giving no product selectivity. Subsequently, we thought of venturing silica having pore diameter in-between the two extremes. We thus, prepared spherical mesoporous silica nano-particles (**Meso-SNP**) of around 800 nm size having pore diameter 2.6 nm with pore volume of 0.52 ccg^{-1} by adopting different synthetic procedure than used for previously mentioned silica materials. Remarkably, on refluxing **1f** with excess HCOOH in presence of **Meso-SNP**, enol-lactone (**2f**) was obtained in (51%) yield (Table 1, entry 4). Being enthued by this consequence, we next prepared another variety of small pore **MCM-41 (SP-MCM-41)** with pore diameter 3.0 nm and pore volume 0.39 ccg^{-1} by fine tuning the synthetic parameters like temperature, ratio of surfactant to tetraethylorthosilicate (TEOS) concentrations, p^H of the medium etc. to check the effect on product yield on further decreasing the pore volume. However, yield increased only marginally (55%) with this new variation of silica (Table 1, entry 5). This puts a termination to our search for ideal silica material as nanoreactor. Invigorated by this success, we next attempted to screen the other reaction parameters (temperature, solvent etc.) for the formation of enol lactones using the previously optimized nanoreactor, **SP-MCM-41** (Table 1, entry 5). Gratifyingly, by decreasing the quantity of HCOOH from excess to 10 mol%, boosted up the yield from 55% to 84% since pyrimidine formation is greatly prevented (Table 1, entry 6). Temperature dependence on the yield of enol lactone (**2f**) to the pyrimidine (**P**) was probed with the same test reaction with 10 mol% of catalyst HCOOH, **SP-MCM-41** as nanoreactor (40 mg) in H_2O. The reaction performed best when the temperature is 80 °C (Table 1, entry 7). However, the reaction did not proceed at 70 °C (Table 1, entry 8). Again, in absence of silica, neither the enol lactone nor the pyrimidine derivative was formed at 80 °C even in presence of excess HCOOH (Table 1, entry 9). This essentially reflects the role of confined space inside the silica mesopore in endorsing such reactions at a relatively lower temperature. Screening of the reaction conditions further established that the yield decreased substantially with stronger inorganic acids as they required recurrent work-up procedures, neutralization steps and extensive chromatographic purification (Table 1, entries 10-14). However, relatively weaker acids afforded better yield because of their less extensive work-up (Table 1, entries 7, 15-18). Therefore, we found that HCOOH is the most efficient catalyst for this reaction among all the screened Brønsted acids. The reaction was unsuccessful in common organic solvents like DMSO, toluene, ACN, EtOH, acetone and DCM which verified that water was indispensable for this transformation and 80 °C as the most effective reaction temperature (Table 1, entries 7). We conducted the reaction in presence of varied amount of **SP-MCM-41** from 40 mg to 5 mg keeping the reaction time unaltered (Table 1, entries 7, 20-22). Since at 80 °C pyrimidine formation is totally stopped, so if we decrease the amount of silica from 40 mg to 5 mg only the yields of enol-lactone gradually decreases (93%–19%) if the reaction time is fixed. Therefore, 40 mg **SP-MCM-41** was optimum amount since increasing amount to more than 40 mg did not improve the yield of enol-lactone. The enol-lactone can also be afforded with porous alumina, however in comparatively less yield than **SP-MCM-41** (Table 1, entry 23). Thus, the reaction parameters given in Table 1, entry 7, were the optimal reaction conditions. Diminishing the amount of HCOOH loading below 10 mol% resulted in incomplete conversion with decreased yield (Table 1, entry 19).

Origin of selectivity

We next turned our attention to find the root why enol lactone is being formed instead of pyrimidine when the reaction is carried out in presence of mesoporous silica. We therefore, primarily wanted to confirm that the reaction is taking place inside the silica pores. To verify this proposition, when chromene with bulkier aromatic group (Ar) like *α*-naphthalene (**1j**), *β*-naphthalene (**1k**) or pyrene derivatives (**1l**) were used, the relative reaction rate decreased, as evident from the time required for the reaction to reach the completion (12 h, 12 h and 16 h respectively; Scheme 2). Therefore, this size-dependent reaction rate provides indirect evidence for the involvement of

Table 1. Screening of Reaction Conditions.[a]

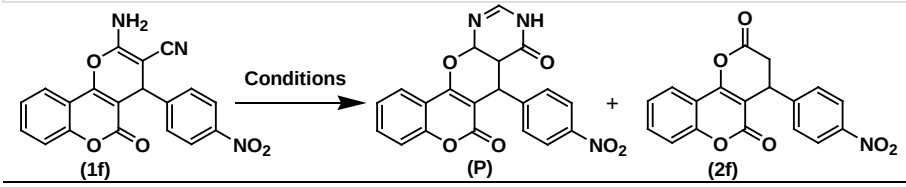

(1f) (P) (2f)

Entry	Type of silica (40 mg)	Textural properties			Catalyst(mol %)	Temp. (°C)	%Yield[b]P	%Yield[b]2f
		SA(m^2g^{-1})	D_p(nm)	V_p(ccg^{-1})				
1	–	–	–	–	HCOOH(excess)	100	>90	<10
2	**LP-MCM-41**	1057	3.56	1.79	HCOOH(excess)	100	>90	<10
3	**Micro-SNP**	739	1.0	0.65	HCOOH(excess)	100	>90	<10
4	**Meso-SNP**	556	2.61	0.52	HCOOH(excess)	100	45	51
5	**SP-MCM-41**	833	3.0	0.39	HCOOH(excess)	100	42	55
6	**SP-MCM-41**	833	3.0	0.39	HCOOH(10)	100	13	84
7	**SP-MCM-41**	833	3.0	0.39	HCOOH(10)	80	trace	93
8	**SP-MCM-41**	833	3.0	0.39	HCOOH(10)	70	–	–
9	–	–	–	–	HCOOH(excess)	80	–	–
10	**SP-MCM-41**	833	3.0	0.39	$HClO_4$ (10)	80	–	25
11	**SP-MCM-41**	833	3.0	0.39	HCl (10)	80	–	27
12	**SP-MCM-41**	833	3.0	0.39	H_2SO_4 (10)	80	–	32
13	**SP-MCM-41**	833	3.0	0.39	HNO_3 (10)	80	–	19
14	**SP-MCM-41**	833	3.0	0.39	H_3PO_4 (10)	80	–	22
15	**SP-MCM-41**	833	3.0	0.39	Lactic (10)	80	–	45
16	**SP-MCM-41**	833	3.0	0.39	Ascorbic (10)	80	–	41
17	**SP-MCM-41**	833	3.0	0.39	PhCOOH (10)	80	–	64
18	**SP-MCM-41**	833	3.0	0.39	AcOH (10)	80	–	79
19	**SP-MCM-41**	833	3.0	0.39	HCOOH (5)	100	trace	70
20	**SP-MCM-41 (20 mg)**	833	3.0	0.39	HCOOH (10)	80	–	65
21	**SP-MCM-41 (10 mg)**	833	3.0	0.39	HCOOH (10)	80	–	41
22	**SP-MCM-41 (5 mg)**	833	3.0	0.39	HCOOH (10)	80	–	19
23	**Meso-Al_2O_3 (40 mg)**	279	4.94	0.29	HCOOH (10)	80	–	76

[a]Reaction conditions: **1f** (1 mmol), silica (40 mg), water (5 mL), time (6 h).

[b]Isolated yields.

the cavity of mesoporous silica. Again, the formation of enol lactones at a relatively low temperature (80 °C) in presence of silica, indicates that the silica meso channel is facilitating the reaction probably by confinement effect. This defines the significance of the confined cavity in promoting such reactions in aqueous media at a relatively low temperature. This proposition is further validated by the non-formation of any enol lactones when the reaction was carried out in presence of non-porous silica at 80 °C probably due to the absence of confinement effect, because, in the case of non-porous materials, the reaction takes place at the external surface of the particles. These facts together with the previously discussed phenomenon of pore size dependent product selectivity reinforce the involvement of silica pores in this reaction. Grounded on these results, we

hypothesized that in case of formation of pyrimidine, the size of the parent chromenes is further increased since one additional ring is formed. However, in case of silica with medium pore size this pathway (pyrimidine formation) is highly prohibited due to the constraint imposed by nanoreactor on rotational and translational motions of the products/intermediates aiding the other pathway to afford the enol lactones having size comparable to the parent chromenes. This may be the reason of product selectivity inside nanoreactor. The diffusion barrier caused by the nanoreactor pores also influences the product and thus also impact product selectivity. These also explicate why silica with very large and very small pore volume and pore diameter could not impart any selectivity for enol lactones.

Effect of heat treatment of silica on product selectivity

Another indirect proof which can support the involvement of silica pore in the reaction and validate the proposed hypothesis is the observed effect of heat treatment of silica on product selectivity. When the silica materials were washed with HCl to remove the TEOS and used as nanoreactor prior to heat treatment, they could not show any selectivity for enol lactones. However, after heating at 600 °C for 8 hours, we reached the above mentioned selectivity for enol lactones. Prior to the heat treatment because of presence of more number of silanol groups, the silica cavity was not sufficiently hydrophobic to promote the reaction preferentially inside the silica pores leaving no selectivity for enol lactones. But after heating it at 600 °C for 8 hours, removal of water from adjacent silanol groups makes the silica pores comparatively more hydrophobic for the organic molecules to enter inside and the reaction to occur favorably inside pores. Therefore, reaction inside pores bestows special selectivity for enol lactones. In Table 2, the effect of heat treatment time on product selectivity is presented which shows that with increasing heat treatment time the selectivity for enol-lactone increases. This may be because of greater extent of silanol condensation and thereby, a decrease in the hydrophilicity inside silica pores promoting the organic molecules to diffuse inside the nanoreactor for size selective catalysis .

Table 2. Effect of heat treatment on enol-lactone selectivity.[a]

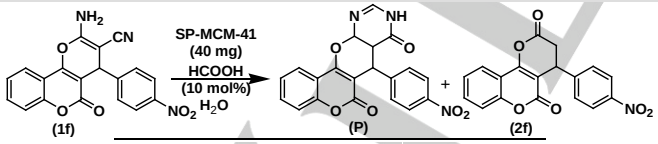

Entry	Time (h)	%Yield[b]P	%Yield[b]2f
1	0	90	<10
2	2	70	26
3	4	46	49
4	6	23	72
5	8	11	85

[a]Reaction conditions: **1f** (1 mmol), water (5 mL), time (6 h), temperature (100 °C), reaction performed with **SP-MCM-41** (40 mg) pre-heated at 600 °C for different time.

[b]Isolated yields.

Substrate Scope for the Synthesis of Enol Lactones

Having obtained the optimized reaction conditions, the scope of the reaction was subsequently investigated, and the representative results are summarized in Scheme 2. Regardless of the electronic nature and the position of substituent on the aromatic ring (Ar) the reaction afforded the corresponding enol lactones in good to excellent yields. When Ar (aromatic) is replaced by R (aliphatic) the reaction was still successful, however, showed a modest decline in yield. It was pleasing to find that cyanide moiety on the aromatic ring was not affected under the present HCOOH mediated hydrolysis condition. Despite the mild conditions, even sterically bulky 1-naphthyl, 2-naphthyl aldehydes and 1-pyrenealdehyde were easily transformed into the desired products in moderate yields. However, the relative reaction rate was decreased with bulkier aldehydes as evident from the reaction completion time. Moreover, much to our satisfaction, the present protocol is mild enough to sustain both the lactone rings in the product as well as acid-sensitive functional groups. In order to guarantee a high flexibility of substitution patterns we addressed the synthesis of enol lactones from *α*- and *ß*-naphthol-4*H*-pyrans (Scheme 3). The structures of enol lactones were confirmed unambiguously from X-ray single crystal analysis of four distinct compounds **4j**, **4l**, **4t**, **4u**. ORTEP plots of **4j** (**CCDC 1408025**), **4l** (**CCDC 1408026**), **4t** (**CCDC 1407896**) and **4u** (**CCDC 1407897**) are given in Figure 6. The scope of this reaction was subsequently extended to *bis* enol lactone systems (Scheme 4).

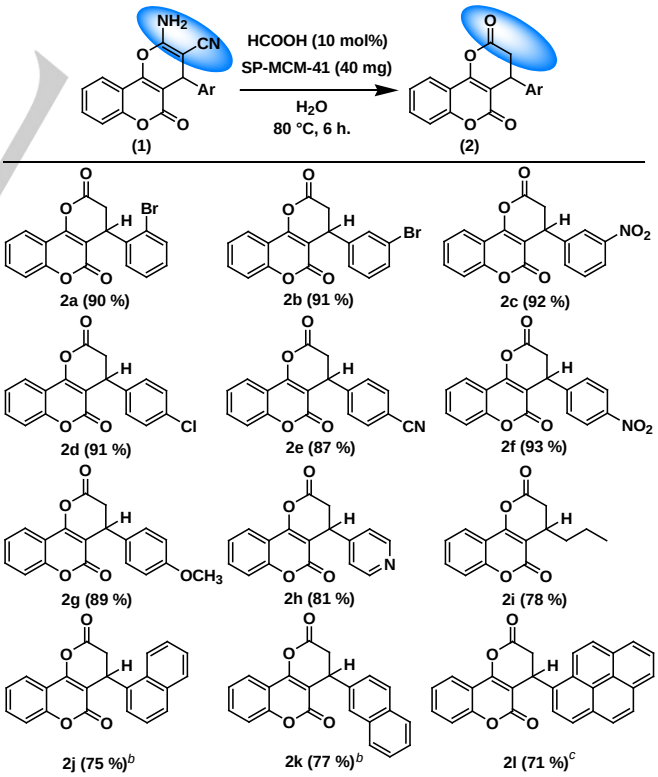

Reaction conditions: [a]Pyran **1** (1 mmol), **SP-MCM-41** (40 mg) and 10 mol% HCOOH catalyst in water (5 mL) was heated at 80 °C for 6 h. [b]time: 12 h. [c]time: 16 h. [d] Isolated yields.

Scheme 2. One-pot Synthesis of Enol Lactones.

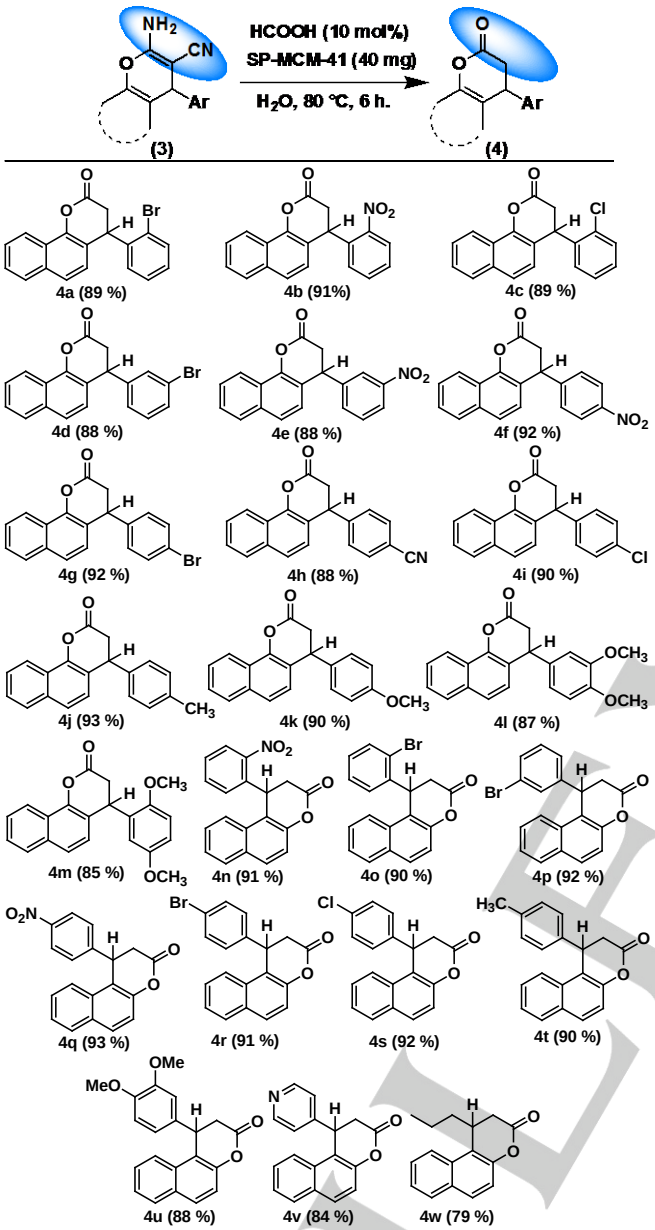

Reaction conditions: [a]Pyran **3** (1 mmol), **SP-MCM-41** (40 mg) and 10 mol% HCOOH catalyst in water (5 mL) was heated at 80 °C for 6 h. [b]Isolated yields.

Scheme 3. Substrate Scope of Enol Lactones.

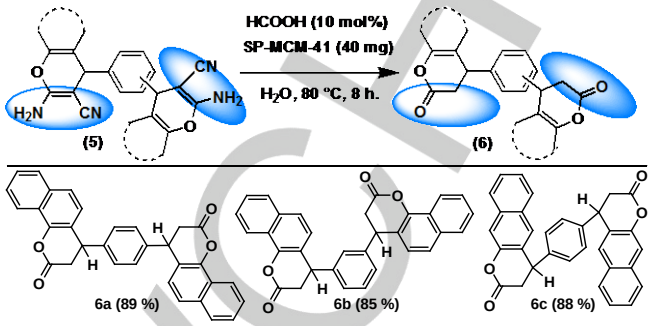

Reaction conditions: [a]Pyran **5**(1 mmol), **SP-MCM-41**(40 mg) and 10 mol% HCOOH catalyst in water (5 mL) was heated at 80 °C for 8 h. [b]Isolated yields.

Scheme 4. Synthesis of *bis* Enol Lactones.

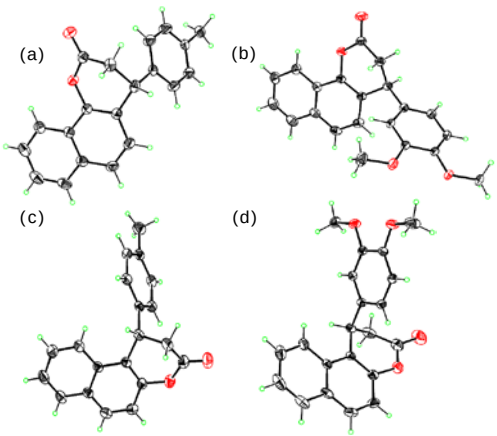

Figure 6. ORTEP representation of (a) **4j** (**CCDC 1408025**), (b) **4l** (**CCDC 1408026**), (c) **4t** (**CCDC 1407896**) and (d) **4u** (**CCDC 1407897**) (thermal ellipsoids at 50% probability in all cases).

Synthesis of δ-keto acids

Based on the above promising results, we thought to further extend the reaction time to monitor any change in the nature of the product. Inspiringly when continued the reaction of **1** with HCOOH for 20 h, we observed an unprecedented reactivity that provided the δ-keto acids (**7**) through triple hydrolysis/decarboxylation/double hydrolysis/double ring opening/tautomerization/decarboxylation cascades, thus unfolding an unrecognized opportunity for their synthesis. Upon the observation of the serendipitous reaction sequences, we shout that this is the first generalized report for the synthesis of δ-keto acids (Scheme 5).

Till date no general scheme for their synthesis has been reported and only a few isolated examples are available as side products.[41] It further demands to be the simplest approach to be

adopted by the scientific community. The final structure of compound **7f** was confirmed by X-ray crystallographic analysis (**CCDC 1407898**) (Figure 7).

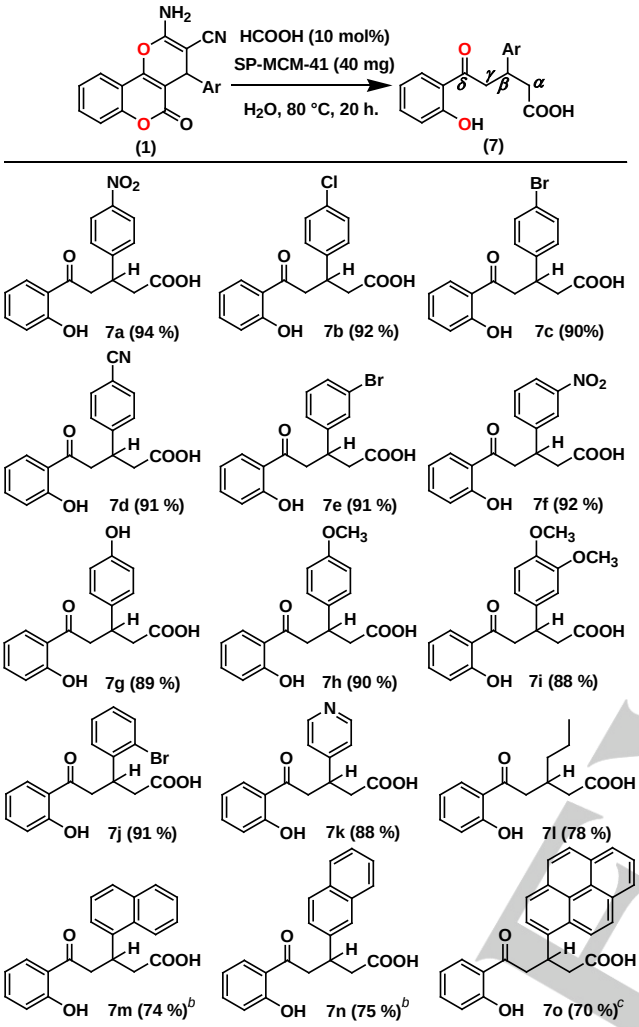

Reaction conditions: [a]Pyran **1** (1 mmol), **SP-MCM-41** (40 mg) and 10 mol% HCOOH catalyst in water (5 mL) was heated at 80 °C for 20 h. [b]time:30 h.[c]time:42 h. [d]Isolated yields.

Scheme 5. Synthesis of δ-keto acids.

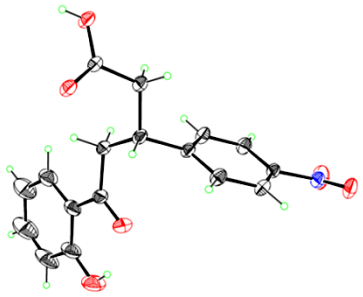

Figure 7. ORTEP Representation of **7f** (**CCDC 1407898**) (thermal ellipsoids at 50% probability).

NMR Study to Monitor Time-Dependent Conversion of Enol Lactone to δ-Keto Acid

The time-dependent conversion of enol lactone (**2b**) to δ-keto acid (**7e**) was carefully monitored by taking ^{1}H NMR spectra of crude reaction mixture. The ^{1}H NMR spectra taken at 6, 9, 12, 15 and 20 h showed that the integration of benzylic C-H peak of enol lactone (Figure 8, red dot) gradually diminished and that of -OH peak of δ-keto acid gradually intensified (Figure 10, blue star) in the crude ^{1}H NMR spectra.

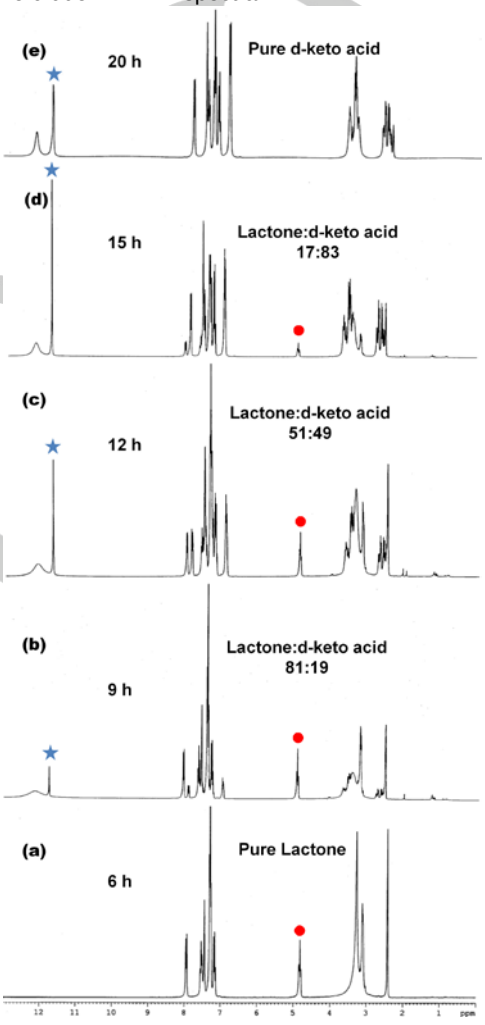

Figure 8. ^{1}H NMR monitoring of the conversion of lactone (**2b**) (red ball) to δ-keto acid (**7e**) (blue star).

Control Experiment

Unlike compound **1** in case of compound **3** even after 48 h, no ring opened product (**8**) was formed (Scheme 6). In case of pyran (**1**) the conversion from enol lactone (**2**) to δ-keto acid (**7**) goes via ß-keto acid (**D**) (Scheme 7) which is easily decarboxylated and subsequently converted to δ-keto acid. However, in case of pyran **3** to acribe the non-formation of (**8**), we heated the reaction mixture at 80 °C with piperadine and isolated the compound **9**. The interpretation of the above results indicates that in **8** the carboxylic acid is not easily decarboxylated and it prefers to stay as stable 6-membered

lactone. When piperidine is added the equilibrium is shifted towards right since the free carboxylic acid forms amide resulting compound **9**. The formation of compound **9** was unambiguously confirmed by X-ray crystal structure (**CCDC 1408296**) (Scheme 6).

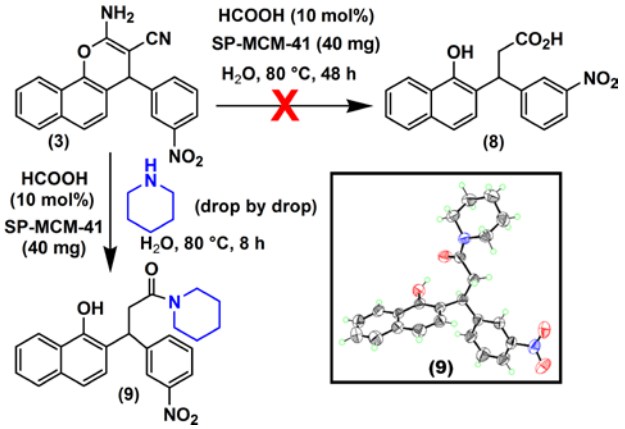

Scheme 6. Control Experiment.

Plausible mechanism

A plausible synthetic mechanistic route, underpinning the formation of enol lactones and *δ*-keto acids is depicted in Scheme 7. Our approach could comprise the relay processes of the following domino sequences: three sequential hydrolyses, followed by decarboxylation to form enol lactone (**2**). This enol lactone undergoes double hydrolysis followed by ring opening of dual lactone ring to form intermediate **D**. **D** endures tautomerization and finally decarboxylation to form *δ*-keto acid (**7**). Notably, this is the first report of tandem triple hydrolysis/decarboxylation/double hydrolysis and double ring opening/tautomerization/decarboxylation to afford *δ*-keto acids.

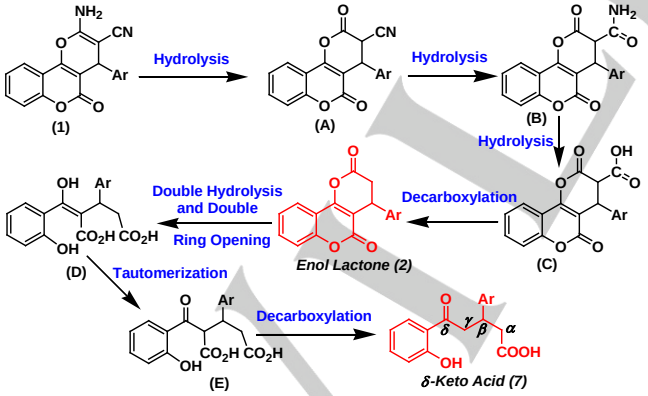

Scheme 7. Plausible Reaction Pathway.

CONCLUSIONS

In summary, we observed an unprecedented sharp product shape selectivity in the hydrolysis/decarboxylation reaction sequences of chromene with formic acid within the mesoporous pores of MCM-41 nanoreactor in liquid phase. When the reaction occurs inside the pores of MCM-41 nanoreactor, the product switches from pyrimidine to enol lactones and *δ*-keto acids. In case of formation of pyrimidine the size of the parent chromenes is further increased since one additional ring is formed. Inside the silica pore, this pathway is highly prohibited due to the constraint imposed by nanoreactor on rotational and translational motions of the products/intermediates aiding the other pathway to afford the enol lactones having size comparable to the parent chromenes. This may be the reason of product selectivity inside nanoreactor. The diffusion barrier caused by the nanoreactor pores also influences the product egress and thus also impact product selectivity. The shape/size selectivity in liquid medium is a much desired effect. Moreover, this is a new mild and metal-free tandem hydrolysis/decarboxylation methodology that can override the existing procedures and subsequently persuade synthetic applications of pyrano-chromene and benzo-chromene in organic chemistry towards the synthesis of biologically relevant coumarin and naphthalene-fused enol lactones. The reaction described here is a rare successful example of enol lactones synthesis in water. Further, the present protocol is mild enough to sustain both the lactone rings in the product as well as acid-sensitive functional groups. More importantly, the import of these discoveries extends beyond simply providing a new synthetic strategy for enol lactones. Finally, we observed an unprecedented reactivity that provide the *δ*-keto acids through an intramolecular tandem triple hydrolysis/decarboxylation/double hydrolysis/double ring opening/tautomerization/decarboxylation, thus unfolding an unrecognized opportunity for their synthesis. This is the first generalized report for the synthesis of *δ*-keto acids. We hope that these reactions will find use outside the academic environment for the synthesis of medicinally important molecular structures.

Acknowledgements

We would also like to thank CAS-V (UGC), DST-FIST and DST-PURSE, Department of Chemistry, University of Calcutta, for funding as departmental projects.

Keywords: mesoporous silica nanoreactor, size/shape selectivity, cascade reaction, enol lactones, *δ*-keto acids

1. a) C. H. Tung, L. Z. Wu, L. P. Zhang, H. R. Li, X. Y. Yi, K. Song, M. Xu, Z. Y. Yuan, J. Q. Guan, H. W. Wang, Y. M. Ying, X. H. Xu, *Pure Appl. Chem.* **2000**, *72*, 2289-2298; b) F. Vögtle, *Supramolecular Chemistry*, Wiley, New York **1991**; c) J. L. Lehn, *Angew. Chem. Int. Ed. Engl.* **1988**, *27*, 89-112; d) H. J. Schneider, Dürr H. (Eds.), *Frontiers in Supramolecular Organic Chemistry and Photochemistry*, VCH, Weinheim, Germany, **1991**; e) V. Balzani, F. Scandola, *Supramolecular Photochemistry*, Prentice-Hall, New York, **1991**; f) X. Qi, X. Li, B. Chen, H. Lu, L. Wang, G. He, *ACS Appl. Mater. Interfaces* **2016**, *8*, 1922−1928.
2. M. P. -Lorenzo, B. Vaz, V. Salgueiriño, M. A. C. Duarte, *Chem. Eur. J.* **2013**, *19*, 12196–12211.
3. a) Z. Chen, Z. M. Cui, P. Li, C. Y. Cao, Y. L. Hong, Z. y. Wu, W. G. Song, *J. Phys. Chem. C* **2012**, *116*, 14986−14991; b) Y. Ai, X. Li, Y. Ji, W. G. Song, Y. Luo, *J. Phys. Chem. C* **2016**, *120*, 10244−10251.

4. a) A. Y. Khodakov, R. Bechara, A. C. Griboval, *Stud. Surf. Sci. Catal.* **2002**, *142*, 1133-1140; b) L. Wei, Y. Zhao, Y. Zhang, C. Liu, J. Hong, *J. Catal.* **2016**, *340*, 205-218; c) A. M. Saib, M. Claeys, E. V. Steen, *Catal. Today* **2002**, *71*, 395-402; d) H. Xiong, Y. Zhang, K. Liew, J. Li, *J. Mol. Catal. B: Enzym.* **2008**, *295*, 68-76; e) J. S. Jung, S. W. Kim, D. J. Moon, *Catal. Today* **2012**, *185*, 168-174; f) I. T. Ghampson, C. Newman, L. Kong, E. Pier, K. D. Hurley, *Appl. Catal. A: Gen.* **2010**, *388*, 57-67; g) C. Liu, C. Cao, J. Liu, X. Wang, Y. Zhuab, W. Song, *J. Mater. Chem. A* **2017**, *5*, 17464-17469; h) K. J. Datta, M. B. Gawande, K. K. R. Datta, V. Ranc, J. Pechousek, M. Krizek, J. Tucek, R. Kale, P. Pospisil, R. S. Varma, T. Asefa, G. Zoppellaro, R. Zboril, *J. Mater.Chem*. *A* **2016**, *4*, 596-604.

5. a) A. T. Dickschat, F. Behrends, M. Bühner, J. Ren, M. Weiß, H. Eckert, A. Studer, *Chem. Eur. J.* **2012**, *18*, 16689-16697; b) I. I. Slowing, B. G. Trewyn, V. S. Y. Lin, *J. Mater. Chem.* **2010**, *20*, 7924-7937; c) S. E. Hankari, A. E. Kadib, A. Finiels, A. Bouhaouss, J. J. E. Moreau, C. M. Crudden, D. Brunel, P. Hesemann, *Chem. Eur. J.* **2011**, *17*, 8984-8994; d) D. Brunel, N. Bellocq, P. Sutra, A. Cauvel, M. Lasperas, P. Moreau, F. Di Renzo, A. Galarneau, F. Fajula, *Coord. Chem. Rev*. **1998**, *178*, 1085-1108; e) A. Walcarius, L. Mercier, *J. Mater. Chem*. **2010**, *20*, 4478-4511; f) A. Quach, V. Escax, L. Nicole, P. Goldner, O. Guillot-Noel, P. Aschehoug, P. Hesemann, J. Moreau, D. Gourier, C. Sanchez, *J. Mater. Chem*. **2007**, *17*, 2552-2560; g) Z. Chen, Z. M. Cui, F. Niu, L. Jiang, W. G. Song, *Chem. Commun*. **2010**, *46*, 6524-6526.

6. a) X. Liu, Y. Maegawa, Y. Goto, K. Hara, S. Inagaki, *Angew. Chem. Int. Ed.* **2016**, *55*, 7943-7947; *Angew. Chem.* **2016**, *128*, 8075–8079; b) S. Inagaki, S. Guan, Y. Fukushima, T. Ohsuna, O. Terasaki, *J. Am. Chem. Soc.* **1999**, *121*, 9611–9614; c) N. Mizoshita, T. Tania, S. Inagaki, *Chem. Soc. Rev.* **2011**, *40*, 789−800; d) J. C. Anthony , H. T. Mark , L. Ming-Yung , G. J. Se, A. D. James, L. S. Susannah, *ACS Catal.* **2011**, 1, 719–728; e) S. Norsic, C. Larabi, M. Delgado, A. Garron, A. de Mallmann, C. Santini, K. C. Szeto, J. –M. Basset, M. Taoufik, *Catal. Sci. Technol.* **2012**, *2*, 215–219; f) C. Baleizão, B. Gigante, D. Das, M. Álvaro, H. Garcia, A. Corma, *J. Catal.* **2004**, *223*, 106-113; g) Y. Zhu, T. Nakanishi, K. Kanamori, K. Nakanishi, S. Ichii, K. Iwaida, Y. Masui, T. Kamei, T. Shimada, A. Kumamoto, Y. H. Ikuhara, M. Jeon, G. Hasegawa, M. Tafu, C. W. Yoon, T. Asefa, *ACS Appl. Mater. Interfaces* **2017**, *9*, 36-41; h) T. Asefa, M. Kruk, N. Coombs, H. Grondey, M. J. MacLachlan, M. Jaroniec, G. A. Ozin, *J. Am. Chem. Soc.* **2003**, *125*, 1662-1673.

7. a) Y. Liu, D. Shen, G. Chen, A. A. Elzatahry, M. Pal, H. Zhu, L. Wu, J. Lin, D. A. Dahyan, W. Li, D. Zhao, *Adv. Mater.* **2017**, *29*, 1702274 (1-8); b) Z. Zhang, X. Wei, Yan Yao, Z. Chen, A. Zhang, W. Li, W. D. Wu, Z. Wu, X. D. Chen, and D. Zhao, *Small* **2017**, *1702243* (1-8); c) A. Corma, H. Garcia, *Top. Catal.* **2008**, *48*, 8-31; d) T.Yokoi, Y. Kubota, T. Tatsumi, *Appl. Catal. A* **2012**, 421-422, 14–37; e) X. Meng, T. Yokoi, D. Lu, T. Tatsumi, *Angew. Chem. Int. Ed.* **2007**, *46*, 7796-7798; *Angew. Chem.* **2007**, *119*, 7942-7944; f) K. Koh, M. Jeon, C. W. Yoon, T. Asefa, *J. Mater. Chem. A* **2017**, *5*, 16150-16161; g) S. Y. Chen, C. Y. Tang, W. T. Chuang, J. J. Lee, C. Y. Tang, J. C. C. Chan, C. Y. Lin, Y. C. Liu. S. Cheng, *Chem. Mater.* **2008**, *20*, 3906–3916; h) G. Graffius, F. Bernardoni, A. Y. Fadeev, *Langmuir* **2014**, *30*, 14797–14807; i) H. S. Zhang, R. H. Jin, H. Yao, S. Tang, J. L. Zhuang, G. Liu, H. X. Li, *Chem.Commun.* **2012**, *48*, 7874–7876; j) S. Y. Chen, C. Y. Huang, T. Yokoi, C. Y. Tang, S. J. Huang, J. -J. Lee, J. C. C. Chan, T. Tatsumi, S. Cheng, *J. Mater. Chem.* **2012**, *22*, 2233-2243.

8. a) F. Chen, C. Kreyenschulte, J. Radnik, H. Lund, A. E. Surkus, K. Junge, M. Beller, *ACS Catal.* **2017**, 7, 1526-1532; b) N. Mangu, H. M. Kaiser, A. Kar, A. Spannenberg, M. Beller, M. K. Tse, *Tetrahedron* **2008**, *64*, 7171-7177; c) Y. Han, D. Zhang, L. L. Chng, J. Sun, L. Zhao, X. Zou, J. Y. Ying, *Nature Chemistry* **2009**, *1*, 123–127; d) M. E. Davis, *Nature* **2002**, *417*, 813-821; e) H. Yang, Z. Ma, T. Zhou, W. Zhang, J. Chao, Y. Qin, *ChemCatChem* **2013**, *5*, 2278-2287; f) H. Yang, G. Li, Z. Ma, *J. Mater. Chem*. **2012**, *22*, 6639-6648; g) S. Li, X. Jiao, H. Yang, *Langmuir* **2013**, *29*, 1228−1237.

9. a) A. Corma, H. Garcia, *Adv.Synth.Catal.* **2006**, *348*, 1391–1412; b) M. Alvaro, A. Corma, D. Das, V. Fornes, H. Garcia, *J. Catal.* **2005**, *231*, 48-55; c) C. del Pozo, A. Corma, M. Iglesias, F. Sanchez, *Green Chem.* **2011**, *13*, 2471-2481; d) V. Polshettiwar, D. Cha, X. Zhang, J. M. Basset, *Angew. Chem. Int. Ed.* **2010**, *49*, 9652-9656; *Angew. Chem.* **2010**, *122*, 9846-9850; e) Y. Hao, Y. Chong, S. Li, H. Yang, *J. Phys. Chem. C* **2012**, *116*, 6512−6519; f) J. Gao, X. Zhang, Y. Lu, S. Liu, J. Liu, *Chem. Eur. J.* **2015**, *21*, 7403-7407; g) R. G. Kadam, A. K. Rathi, K. Cepe, R. Zboril, R. S. Varma, M. B. Gawande, R. V. Jayaram, *ChemPlusChem* **2017**, *82*, 467-473; h) R. Singh, R. R. Bapat, L. Quen, H. Feng, V. Polshettiwar, *ACS Catal*. **2016**, *6*, 2770−2784; i) A. S. L. Thankamony, C. Lion, F. Pourpoint, B. Singh, A. J. Perez Linde, D. Carnevale, G. Bodenhausen, H. Vezin, O. Lafon, V. Polshettiwar, *Angew. Chem. Int. Ed.* **2015**, *54,* 2190-2193; *Angew. Chem*. **2015**, *127*, 2218 –2221; j) D. Wang, L. Etienne, M. Echeverria, S. Moya, D. Astruc, *Chem. Eur. J*. **2014**, *20*, 4047-4054.

10. a) M. Buaki-Sogo, H. Garcia, C. Aprile, *Catal. Sci. Technol.* **2015**, *5*, 1222-1230; b) G. Budroni, A. Corma, H. García, A. Primo, *J. Catal.* **2007**, 251, 345–353; c) M. Waki, N. Mizoshita, T. Ohsuna, T. Tania, S. Inagaki, *Chem. Commun.* **2010**, *46*, 8163−8165; d) P. Borah, X. Ma, K. T. Nguyen, Y. Zhao, A Vanadyl, *Angew. Chem. Int. Ed.* **2012**, *51*, 7756-7761; *Angew. Chem.* **2012**, *124*, 7876-7881; e) N. R. Shiju, A. H. Alberts, S. Khalid, D. R. Brown, G. Rothenberg, *Angew. Chem. Int. Ed.* **2011**, *50*, 9615–9619; *Angew. Chem.* **2011**, *123*, 9789–9793; e) K. Sugino, N. Oya, N. Yoshie, M. Ogura, *J. Am. Chem. Soc.* **2011**, *133*, 20030–20032; f) V. Polshettiwar, D. Cha, X. Zhang, J. M. Basset, *Angew. Chem. Int. Ed.* **2010**, *49*, 9652–9656; *Angew. Chem.* **2010**, *122*, 9846-9850; g) K. Zhang, L. L. Xu, J. G. Jiang, N. Calin, K. F. Lam, S. J. Zhang, H. H. Wu, G. D. Wu, B. Albela, L. Bonneviot, P. Wu, *J. Am. Chem. Soc.* **2013**, *135*, 2427−2430; h) B. M. Weckhuysen, R. R. Rao, P. Bodart, G. Debras, O. Collart, P. V. D. Voort, E. F.Vansant, R. A. Schoonheydt, *Chem. Eur. J.* **2000**, *6*, 2960-2970; i) H. Zhao, W. He, R. Yao, M. Cai, *Adv. Synth. Catal.* **2014**, *356*, 3092–3098; j) S. Okada, K. Mori, T. Kamegawa, M. Che, H. Yamashita, *Chem. Eur. J.* **2011**, *17*, 9047–9051.

11. a) S. Shylesh, A. Wagner, A. Seifert, S. Ernst, W. R. Thiel, *Chem. Eur. J.* **2009**, *15*, 7052–7062; b) C. T. Kresge, M. E. Leonowicz, W. J. Roth, J. C. Vartuli, J. S. Beck, *Nature* **1992**, *359*, 710-712; c) N. Ishito, H. Kobayashi, K. Nakajima, Y. Maegawa, S. Inagaki, K. Hara, A. Fukuoka, *Chem. Eur. J.* **2015**, *21*, 15564-15569; d) E. –Y. Jeong, C. R. Lim, H. Jin, S. E. Park, *Chem. Commun.* **2012**, *48*, 3079-3081; e) Y. Furukawa, M. Ogura, *J. Am. Chem. Soc.* **2014**, *136*, 119-121; f) X. Z. Shu, S. C. Nguyen, Y. He, F. Oba, Q. Zhang, C. Canlas, G. A. Somorjai, A. P. Alivisatos, F. D. Toste, *J. Am. Chem. Soc.* **2015**, *137*, 7083–7086; g) K. Liu, R. Jin, T. Cheng, X. Xu, F. Gao, G. Liu, H. Li, *Chem. Eur. J.* **2012**, *18*, 15546-15553; h) X. Xia, J. Meng , H. Wu , T. Cheng, G. Liu, *Chem. Commun*. **2017**, *53*, 1638-1641.

12. a) L. Wei, Y. i Zhao, Y. Zhang, C. Liu, J. Hong, H. Xiong, J. Li, *J. Catal.* **2016**, *340*, 205-218; b) K. Cheng, M. Virginie, V. V. Ordomsky, C. Cordier, P. A. Chernavskii, M. I. Ivantsov, S. Paul, Y. Wang, A. Y. Khodakov, *J. Catal*. **2015**, *328*, 139-150.

13. a) H. F. Xiong, Y. H. Zhang, K. Y. Liew, J. L. Li, *J. Mol. Catal. A: Chem*. **2008**, *295*, 68-76; b) G. Prieto, A. Martinez, R. Murciano, M. A. Arribas, *Appl. Catal. A Gen*. **2009**, *367*, 146-156; c) H. F. Xiong, Y. H. Zhang, S. G. Wang, K. Y. Liew, J. L. Li, *J. Phys. Chem. C* **2008**, *112*, 9706–9709.

14. a) Y. Wang, N. Sua, L. Ye, Y. Ren, X. Chen, Y. Du, Z. Li, B. Yue, S. C. E. Tsang, Q. Chen, H. He, *J. Catal.* **2014**, *313*, 113–126; b) D. J. Mihalcik, W. Lin, *ChemCatChem* **2009**, *1*, 406–413; c) M. K. Kidder, A. L. Chaffee, M. H. T. Nguyen, A. C. Buchanan, *J. Org. Chem*. **2011**, *76*, 6014–6023; d) K. D. M. Harris, J. M. Thomas, *ChemCatChem* **2009** , *1*, 223–231; e) L. Zhao, Y. Li, P. Yu, X. Han,

J. He, *ACS Catal*. **2012**, *2*, 1118−1126; f) R. Raja, J. M. Thomas, M. D. Jones, B. F. G. Johnson, D. E. W. Vaughan, *J. Am. Chem. Soc*. **2003**, *125*, 14982-14983; g) J. M. Fraile, N. Garcia, C. I. Herrerias, *ACS Catal*. **2013**, *3*, 2710−2718; h) E. Pump, Z. Cao, M. K. Samantaray, A. Bendjeriou-Sedjerari, L. Cavallo, J. M. Basset, *ACS Catal*. **2017**, *7*, 6581−6586; i) H. Yang, L. Zhang, L. Zhong, Q. Yang, C. Li, *Angew. Chem. Int. Ed*. **2007**, *46*, 6861–6865; j) Y. Yang, Z. Weng, S. Muratsugu, N. Ishiguro, S. i. Ohkoshi, M. Tada, *Chem. Eur. J.* **2012**, *18*, 1142–1153; k) H. Cao, X. H. Zhu, D. Wang, Z. Sun, Y. Deng, X. F. Hou, D. Zhao, *ACS Catal*. **2015**, *5*, 27 − 33; l) T. Kawasaki, Y. Araki, K. Hatase, K. Suzuki, A. Matsumoto, T. Yokoi, Y. Kubota, T. Tatsumi, K. Soai, *Chem. Commun.* **2015**, *51*, 8742-8744; m) C. E. Song, D. H. Kim, D. S. Choi, *Eur. J. Inorg. Chem.* **2006**, 2927–2935; n) Y. Yang, R. M. Rioux, *Green Chem*. **2014**, *16*, 3916–3925; o) J. L. Defreese, S. J. Hwang, A. N. G. Parra-Vasquez, A. Katz, *J. Am. Chem. Soc*. **2006**, *128*, 5687-5694; p) H. Q. Yang, Y. Z. Chong, X. K. Li, H. Ge, W. B. Fan, J. G. Wang, *J. Mater. Chem*. **2012**, *22*, 9069-9076; q) C. Liu, J. Liu, S. Yang, C. Cao, W. Song, *ChemCatChem* **2016**, *8*, 1279-1282; r) X. Wang, M. Li, C. Cao, C. Liu, J. Liu, Y. Zhu, S. Zhang, W. Song, *ChemCatChem* **2016**, *8*, 3224-3228.

15. P. J. Dunn, *Chem. Soc. Rev*. **2012**, *41*, 1452-1461.
16. R. A. Sheldon, I. Arends, U. Hanefeld, *Green Chemistry and Catalysis,* Wiley-VCH: Weinheim, Germany, **2007**, 1.
17. D. S. Bose, L. Fatima, H. B. Mereyala, *J. Org. Chem.* **2003**, *68*, 587-590.
18. a) S. Bertelsen, K. A. Jorgensen, *Chem. Soc. Rev*. **2009**, *38*, 2178-2189; b) D. G. Blackmond, A. Armstrong, V. Coombe, A. Wells, *Angew. Chem. Int. Ed*. **2007**, *46*, 3798-3800; *Angew. Chem.* **2007**, *119*, 3872-3874; c) X. Tian, K. Jiang, J. Peng, W. Du, Y. -C. Chen, *Org. Lett*. **2008**, *10*, 3583-3586; d) Y. Zhang,Y. -K. Liu, T. -R. Kang, Z. -K. Hu, Y. -C. Chen, *J. Am. Chem. Soc*. **2008**, *130*, 2456-2457; e) T. -Y. Liu, H. -L. Cui, Y. Zhang, K. Jiang, W. Du, Z.-Q. He, Y. -C. Chen, *Org. Lett*. **2007**, *9*, 3671-3674; f) M. -L. Shi, G. Zhan, S. -L. Zhou, W. Du, Y. -C. Chen, *Org. Lett*. **2016**, *18*, 6480−6483; g) C. Mukhopadhyay, P. Das, R. J. Butcher, *Org. Lett*. **2011**, *13*, 4664-4667; h) J. Peng, G. -Y. Ran, W. Du, Y. -C. Chen, *Org. Lett*. **2015**, *17*, 4490−4493.
19. J. Alemán, S. Cabrera, *Chem. Soc. Rev.* **2013**, 42, 774-793.
20. a) K. Maruoka, B. List, H. Yamamotoc, L. Z. Gong, *Chem. Comm.* **2012**, *48*, 10703-10703; b) C. Mukhopadhyay, S. Ray, *Tetrahedron Lett*. **2011**, *52*, 6431-6438; c) S. Ray, C. Mukhopadhyay, *Tetrahedron Lett*. **2013**, 54*,* 5078-5082.
21. a) L. N. Ferguson, *Chem. Soc. Rev.* **1975**, *4*, 289-322; b) E. Fujita, Y. Nagao, *Bioorg. Chem*. **1977**, *6,* 187-309**.**
22. a) E. K. Seo, M. C. Wani, M. E. Wall, H. Navarro, R. Mukherjee, N. R. Farnsworth, A. D. Kinghorn, *Phytochemistry* **2000**, *55*, 35-42; b) A. Mazumder, S. Wang, N. Neamati, M. Nicklaus, S. Sunder, J. Chen, G. W. A. Milne, W. G. Rice, T. R. Jr. Burke, Y. Pommier, *J. Med. Chem*. **1996**, *39*, 2472-2481.
23. S. Wang, G. W. A. Milne, X. Yan, I. J. Posey, M. C. Nicklaus, L. Graham, W. G. Rice, *J. Med. Chem*. **1996**, *39*, 2047-2054.
24. Y. J. Lee, T. H. Tseng, Y. J. Lee, *Synthesis* **2001**, 2247-2254.
25. a) H. Miao, Z. Yang, *Org. Lett.* **2000**, *2*, 1765-1768; b) P. Kumar, M. S. Bodas, *Org. Lett.* **2000**, *2*, 3821-3823.
26. R. S. Thelingwani, K. Dhansay, P. Smith, K. Chibale, C. M. Masimirembwa, *Xenobiotica* **2012**, *42*, 989-1000.
27. X. A. Huang, R. Yang, X. Cai, S. Ye, Y. Hu, *J. Mol. Struct*. **2007**, *830*, 100-105.
28. T. Murakami, N. Takada, W. Hehre, *Bioorg. Med. Chem. Lett*. **2008**, *18*, 4547-4549.
29. X. Huang, H. Jiang, G. Hao, *Fitoterapia*. **2009**, *80*, 173-176.
30. K. Otoguro, F. Kuno, S. Omura, *Pharmacology therapeutics* **1997**, *76*, 45-54.
31. a) G. Speranza, C. F. Morelli, P. Manitto, *Synthesis* **2000**, *1*, 123-126; b) B. L. Zhao, D. M. Du, *Tetrahedron: Asymmetry* **2014**, *25,* 310-317; c) K. Itoh, S. Kanemasa, *Tetrahedron Lett.* **2003**, *44*, 1799-1802; d) S. Ahadi, M. Zolghadr, H. R. Khavasi, *Org. Biomol. Chem*. **2013**, *11*, 279-286; e) J. M. Khurana, V. Kanika, *Tetrahedron Lett.* **2011**, *52*, 3666-3669; f) F. K. Mohammed, A. Y. Soliman, A. Ssawy, M. G. Badre, *J. Chem. Pharm. Res*. **2009**, *1*, 213-224.
32. a) S. J. Tu, J. F. Zhou, P. J. Cai, H. Wang, J. C. Feng, *Syn. Comm.* **2001**, *31*, 3729-3733; b) I. Yavari, M. Sabbaghan, Z. Hossaini, *Synlett* **2008**, *8*, 1153-1154.
33. a) G. Speranza, A. D. Meo, S. Zanzola, G. Fontana, P. Manitto, *Synthesis* **1997**, 931-936; b) J. Peng, X. Huang, P. -F. Zheng, Y. –C. Chen, *Org. Lett*. **2013**, *15*, 5534–5537; c) M. M. Kandeel, A. M. Kamal, E. K. A. Abdelall, H. A. H. Elshemy, *Org. Chem. Indian J.* **2012**, *8*(9), 342-348.
34. K. Itoh, M. Hasegawa, J. Tanaka, S. Kanemasa, *Org. Lett*. **2005**, *7*, 979-981.
35. S. R. Yetra, T. Roy, A. Bhunia, D. Porwal, A. T. Biju, *J. Org. Chem*. **2014**, *79*, 4245-4251.
36. M. Nandi, M. Sarkar, K. Sarkar, A. Bhaumik, *J. Phys. Chem. C* **2009**, *113*, 6839-6844.
37. S. K. Das, M. K. Bhunia, A. Bhaumik, *J. Solid State Chem.* **2010**, *183*, 1326-1333.
38. P. Das, A. Dutta, A. Bhaumik, C. Mukhopadhyay, *Green Chem.* **2014**, *16*, 1426-1435.
39. a) N. R. Kamdar, D. D. Haveliwala, P. T. Mistry, S. K. Patel, *Med. Chem. Res.* **2011**, *20*, 854–864; b) N. R. Kamdar, D. D. Haveliwala, P. T. Mistry, S. K. Patel, *Eur. J. Med. Chem*. **2010**, *45*, 5056-5063; c) A. Agarwal, K. Srinivas, S. K. Puri , P. M. S. Chauhan, *Bioorg. Med. Chem*. **2005**, *13*, 4645–4650; d) A. Ali, G. E. Taylor, K. Ellsworth, G. Harris, R. Painter, L. L. Silver, K. Young, *J. Med. Chem*. **2003**, *46*, 1824–1830; e) N. Sunduru, A. Agawal, S. Katiyar, B. Nishi, N. Goyal, S. Gupta, P. M. S. Chauhan, *Bioorg. Med. Chem*. **2006**, 14, 7706–7715; f) M. N. S. Saudi, M. R. Gaafar, M. Z. El-Azzouni, M. A. Ibrahim, M. M. Eissa, *Med. Chem. Res*. **2008**, 17, 541–563; g) M. B. Deshmukh, S. M. Salunkhe, D. R. Patil, P. V. Anbhule, *Eur. J. Med. Chem*. **2009**, *44*, 2651-2654; h) G. Cecile, D. Douguet, V. Huteau, M. Gilles, M. L. Helene, P. Sylvie, *Bioorg. Med. Chem*. **2008**, *16*, 6075-6085; i) R. Lin, G. Sigmond, P. J. Johnson, S. K. Connolly, E. Wetter, T. V. Binnun, W. V. Hughes, N. B. Murray, S. J. Pandey, M. M. Mazza, A. R. Adams, F. Pesquera, A. M. Steven, *Bioorg. Med. Chem. Lett*. **2009**, *19*, 2333-2337; j) E. P. Falcao, S. da, S. J. Melo, R. M. Srivastava, M. T. Catanho, S. C. Nascimento, *Eur. J. Med. Chem*. **2006**, *41*, 276-282; k) Q. Chen, X. Zhu, L. Jiang, L. M. Yang, G. Fu, *Eur. J. Med. Chem.* **2008**, *43*, 595-603; l) A. Agarwal, R. Ashutosh, N. Goyal, M. S. Chauhana, S. Gupta, *Bioorg. Med. Chem*. **2005**, *13*, 6678-6684.
40. a) S. Ray, A. Bhaumik, A. Dutta, C. Mukhopadhyay, *Catal. Sci. Technol.* **2013**, *3*, 1267-1277; b) S. Ray, P. Das, B. Banerjee, A. Bhaumik, C. Mukhopadhyay, *RSC Adv*. **2015**, *5*, 72745-72754; c) S. Ray, A. Bhaumik, M. Pramanik, C. Mukhopadhyay, *RSC Adv*. **2014**, *4*, 15441-15450; d) S. Ray, P. Das, A. Bhaumik, A. Dutta, C. Mukhopadhyay, *Appl. Catal. A: Gen*. **2013**, *458*, 183–195; e) S. Ray, M. Brown, A. Bhaumik, A. Dutta, C. Mukhopadhyay, *Green Chem*. **2013**, *15*, 1910-1924.
41. S. K. Ray, P. K. Singh, N. Molleti, V. K. Singh, *J. Org. Chem*. **2012**, *77*, 8802-8808.

10.1002/cctc.201701975

10.1002/cctc.201701975

Entry for the Table of Contents (Please choose one layout)

Layout 1:

FULL PAPER

Unprecedented sharp product shape selectivity in the hydrolysis/decarboxylation reaction sequences of chromene with formic acid within MCM-41 as nanoreactor in liquid phase affording enol lactones and δ-keto acids.

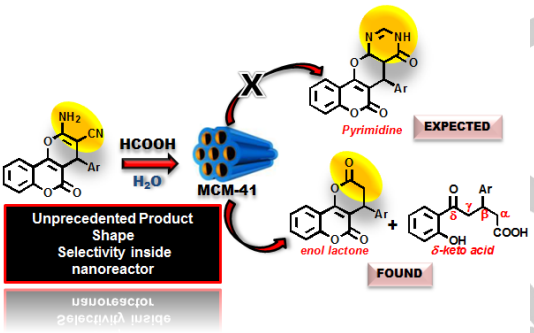

*Paramita Das, Suman Ray, Piyali Bhanja, Asim Bhaumik, Chhanda Mukhopadhyay**

Page No.* – *Page No.

A Serendipitous Observation of Liquid Phase Size Selectivity inside Mesoporous Silica Nanoreactor in the Reaction of Chromene with Formic Acid

Layout 2:

FULL PAPER

*Author(s), Corresponding Author(s)**

Page No.* – *Page No.

Title

Text for Table of Contents